The promoter and signal sequence of staphylococcal enterotoxin B [C. L. Jones and S. A. Khan, *J. Bacteriol.* **166**, 29 (1986)] were amplified from the chromosomal DNA of *S. aureus* S6 with oligonucleotides 5′-AAGAATTCGTATATAAGTTTAGGTGATGT-3′ and 5′-AAGGTACCGGTTGACTCTCTGCTAAAA-3′. The following genes were digested with the indicated restriction enzymes: *seb*, Eco RI and Kpn I; *malE*, Kpn I and Hind III; and *spa*, Hind III and Bam HI. The resulting DNA fragments were cloned between the Eco RI and Bam HI sites of pOS1 (*8*). The recombinant plasmid pSebsp–MalE-Cws was transformed into *S. aureus* OS2 (*7*) and maintained by chloramphenicol selection. The hybrid protein consists of the first 33 residues of Seb, which includes the signal peptide and six residues of the mature sequence fused to the NH_2-terminal lysine of mature MalE. The sorting signal and 13 upstream residues of protein A are fused to the COOH-terminal lysine of MalE with a leucine linker preceding Glu^{477} of protein A. The open reading frame of MalE-Cws was sequenced, revealing a single point mutation that changed Gly^{306} to aspartic acid (G998A transition).

13. J.-M. Ghuysen, *Bacteriol. Rev.* **32**, 425 (1968).
14. C. A. Schindler and V. T. Schuhardt, *Proc. Natl. Acad. Sci. U.S.A.* **51**, 414 (1964).
15. For a typical purification 10^{12} colony-forming units of an exponential *S. aureus* OS2 (pSebsp–MalE-Cws) culture were harvested by 10,000*g* centrifugation from 4 liters of tryptic soy broth. Cells were resuspended in 200 ml of water and extracted with 200 ml of ice-cold acetone:ethanol (1:1) for 15 min [R. P. Novick, *Methods Enzymol.* **204**, 587 (1991)]. After the addition of another 400 ml of water, the cells were washed in 800 ml of STM buffer (0.5 M sucrose, 50 mM tris-HCl, pH 8.0, and 10 mM $MgCl_2$), resuspended in 140 ml of prewarmed STM, and digested with 10 mg of lysostaphin (Applied Microbiology) for 2 hours at 37°C. Protoplasts were collected by 20,000*g* centrifugation for 30 min, and the supernatant (cell wall digest) was filtered, dialyzed against TSM buffer (20 mM tris-HCl, pH 7.5, 200 mM NaCl, and 10 mM mercaptoethanol), and loaded onto 10 ml of amylose resin [T. Ferenci and U. Klotz, *FEBS Lett.* **94**, 213 (1978)] (New England Biolabs). The column was washed with 200 ml of TSM, and MalE-Cws was finally eluted with 10 ml of 10 mM maltose in TSM. The eluate was dialyzed against 50 mM NH_4HCO_3, concentrated by filtration on centriprep-30/centricon-30 membranes (Amikon), and the protein concentration determined by comparison with a standard (MBP-2**, New England Biolabs). A typical purification yielded 0.1 mg of pure MalE-Cws. Purified MalE–Cws (1 μg) was separated on a 10% SDS-PAGE, electroblotted onto Trans-Blot membrane (Bio-Rad), stained (0.25% Brilliant Blue R-250 in 40% methanol), and the excised band subjected to Edman degradation. The NH_2-terminal sequence ESQPVPKI was determined, and reactions were stopped after eight cycles. For rpHPLC purification, 0.3 mg of purified protein was injected (3× 250 μl in 50 mM NH_4HCO_3, 20% glacial acetic acid) onto a rpHPLC column [2.1 mm by 250 mm Shandon Hypersil butyl, 5-μm particle size, eluted with an increasing concentration of acetonitrile, 1% per minute in 0.1% trifluoroacetic acid (TFA)]. MalE-Cws eluted at 56% acetonitrile, 0.1% TFA; the corresponding fraction was dried under vacuum and solubilized in 50 μl of 50% acetonitrile 0.1% formic acid, and 5 μl (100 pmol) were injected into the ion source of an electrospray mass spectrometer (Sciex API III R) and scanned at *m/z* 1000 to 1800. About 40 scans were averaged, and signals were mass measured by means of the multiply charged ion series from the separate introduction of polypropylene glycol for calibration. Deconvolution of the series of multiply charged ions and calculation of protein molecular weight were achieved with the Hypermass computer program. Under standard conditions the accuracy of these mass measurements is 0.01% of the molecular weight. For muramidase digestion, the acetone-ethanol extracted cells were resuspended in STM buffer, pH 6.8, and digested with 10,000 units of mutanolysin [K. Yokogawa, S. Kawata, S. Nishimura, Y. Ikeda, Y. Yoshimura, *Antimicrob. Agents Chemother.* **6**, 156 (1974)] and 100 mg of egg white lysozyme (Sigma) for 12 hours at 37°C. Mutanolysin (Sigma) contains a substantial protease contamination which was inhibited with 2 mM phenylmethylsulfonyl fluoride (PMSF, Sigma) 5 min before the addition of the enzyme to the cells.
16. The optimal temperature and enzyme-to-substrate ratio for tryptic digestion of MalE-Cws were established: 0.3 mg of affinity-purified MalE-Cws was digested with 11 μg of sequencing-grade modified trypsin (Promega) at 25°C for 2 hours in 500 μl of 50 mM NH_4HCO_3. The digestion was stopped by the addition of 120 μl of glacial acetic acid, and portions (2 μg) were removed for SDS-PAGE analysis. After electroblotting of the SDS-PAGE and staining with Brilliant Blue, the bands were excised and analyzed by NH_2-terminal sequencing which yielded the sequence IEEGKLV. The remainder of the trypsin digest was subjected to rpHPLC (*15*). The large MalE-Cws cleavage product eluted at 58% acetonitrile. The corresponding fraction was dried under vacuum, solubilized, and mass measured (*15*).
17. W. W. Navarre and O. Schneewind, *Mol. Microbiol.* **14**, 115 (1994).
18. The 2-min fractions 1 to 5, 6 to 10, 11 to 15, 16 to 20, and 21 to 25 of the rpHPLC run of trypsin-digested MalE-Cws (*16*) were pooled, dried under vacuum, and resuspended in 50 μl of 0.1% TFA. Samples (5 μl each) were injected onto rpHPLC column (Keystone Scientific Betasil C18, 1 mm by 100 mm, 5-μm particle size, 100 Å pore size, linear gradient of acetonitrile 1% per minute in 0.1% TFA), and the effluent was passed directly into the electrospray mass spectrometer. The NH_2- and COOH-terminal peptides with mass 784.3 and 900.5, respectively, were identified in the pooled fractions 1 to 5 and eluted at 25% (NH_2-terminal peptide) or 26% (COOH-terminal peptide) acetonitrile. The remainder of pooled fraction 1 (45 μl) was subjected to rpHPLC (2 mm by 250 mm Shandon Hypersil ODS, 3-μm particle size, linear gradient of acetonitrile 1% per minute in 0.1% TFA); the peptides of interest eluted at 24% (NH_2-terminal peptide) and 27% acetonitrile (COOH-terminal peptide).
19. As determined with a Porton 2090E sequencer, the amounts of amino acids recovered after Edman degradation of the COOH-terminal peptide were 714 pmol (A), 584 pmol (Q), 430 pmol (A), 262 pmol (L), 104 pmol (P), 91 pmol (E), 33 pmol (T), 27 pmol (G), 27 pmol (G), and 23 pmol (G). The yield of amino acids declined rapidly after the sixth cycle [after the cleavage of glutamic acid (E) in the COOH-terminal peptide AQALPETGGG], presumably because the remaining peptides were retained with decreased efficacy on the sequencing filter.
20. H. P. Browder, W.A. Zygmunt, J. R. Young, P. A. Tavoramina, *Biochem. Biophys. Res. Commun.* **19**, 383 (1965); G. L. Sloan, E.C. Smith, J. H. Lancaster, *Biochem. J.* **167**, 293 (1977); P. A. Recsei, A. D. Gruss, R. P. Novick, *Proc. Natl. Acad. Sci. U.S.A.* **84**, 1127 (1987).
21. B. L. M. de Jonge, Y.-S. Chang, D. Gage, A. Tomasz, *J. Biol. Chem.* **267**, 11248 (1992).
22. K. H. Schleifer and O. Kandler, *Bacteriol. Rev.* **36**, 407 (1972).
23. D. J. Tipper and J. L. Strominger, *Proc. Natl. Acad. Sci. U.S.A.* **54**, 1133 (1965).
24. J.-M. Ghuysen, D. J. Tipper, C. H. Birge, J. L. Strominger, *Biochemistry* **4**, 2245 (1965); J.-F. Petit, E. Munöz, J.-M. Ghuysen, *ibid.* **5**, 2765 (1966).
25. J. L. Strominger, K. Izaki, M. Matsuhashi, D. J. Tipper, *Fed. Proc.* **26**, 9 (1967); J. L. Strominger and J.-M. Ghuysen, *Science* **156**, 213 (1967).
26. A. Forsgren, *Acta Pathol. Microbiol. Scand.* **75**, 481 (1969).
27. G. D. Shockman and J. F. Barrett, *Annu. Rev. Microbiol.* **37**, 501 (1983).
28. We thank D. Boyd, S. Daefler, P. Model, and M. Russel for many discussions and critically reading the manuscript. We also thank C. Canzanella, W. W. Navarre, and T. Baba for critical comments on the manuscript. We acknowledge the technical assistance of J. Chuang and P. Abdul-Sayed during these studies. Supported by NIH grant AI 33985 to O.S.

7 October 1994; accepted 21 December 1994

Antigen-Specific Development of Primary and Memory T Cells in Vivo

Michael G. McHeyzer-Williams and Mark M. Davis

The expansion and contraction of specific helper T cells in the draining lymph nodes of normal mice after injection with antigen was followed. T cell receptors from purified primary and memory responder cells had highly restricted junctional regions, indicating antigen-driven selection. Selection for homogeneity in the length of the third complementarity-determining region (CDR3) occurs before selection for some of the characteristic amino acids, indicating the importance of this parameter in T cell receptor recognition. Ultimately, particular T cell receptor sequences come to predominate in the secondary response and others disappear, showing the selective preservation or expansion of specific T cell clones.

Antigen-specific primary and memory helper T cell responses are central to the establishment of protective immunity (*1*). Tracking the fate of these antigen-specific helper T cells in vivo has been a significant technical problem, mainly because of their very low frequencies in normal animals. Whereas ligand binding can be monitored directly in the B cell compartment (*2*), this has not been possible for T cells because of their relatively low affinities (*3*). To overcome this problem, we used the mouse T cell antigen pigeon cytochrome c (PCC), which is restricted by $I\text{-}E^k$ (*4*). T cells that respond to this antigen express a uniform type of αβ T cell receptor (TCR) heterodimer ($V_\alpha 11V_\beta 3$) (*5*). By staining cells with antibodies specific for these V regions

M. G. McHeyzer-Williams, Department of Microbiology and Immunology, Stanford University School of Medicine, Stanford, CA 94305, USA.
M. M. Davis, Department of Microbiology and Immunology and Howard Hughes Medical Institute, Stanford University School of Medicine, Stanford, CA 94305, USA.

(6) as well as for markers of T cell activation (7), we can directly identify, purify, and characterize the very small fraction (less than 0.1%) of responsive T cells.

After the first injection with antigen, a population of helper T cells accumulated expressing $V_\alpha 11V_\beta 3$, low levels of L selectin, and high levels of CD44 (Fig. 1). At the height of the primary response (day 6), there were 5.0×10^4 activated $V_\alpha 11V_\beta 3$ helper T cells in the draining lymph nodes (either L selectin^{lo} or CD44^{hi}; 0.4 ± 0.1% of total helper T cells) (Fig. 1). This represents an increase of 27 times the background levels of activated $V_\alpha 11V_\beta 3$ helper T cells before injection (Fig. 1). These values are dependent on the presence of antigen, because adjuvant alone elicited only a modest increase (1.5 times the background) (Fig. 1). We also monitored the activated $V_\alpha 11^+V_\beta 3^-$ or $V_\alpha 11^-V_\beta 3^+$ helper cells over the same time course and found no significant increase versus the overall cell number. By day 14, only 25% of the antigen-activated subset remained, and after 8 weeks the number of activated cells was less than two times that found in the background (Fig. 1).

After reinjection of antigen, the number of antigen-activated T cells in the draining nodes rose more rapidly, peaking at day 4 (Fig. 1). The response to adjuvant alone was consistently higher than that seen after the first injection but was still only 20% of the response seen with antigen (Fig. 1). The total number of resting and activated helper T cells also increased by a factor of 3 to 4 over this time span, as it did with the primary response. By day 14, only 30% of the antigen-activated cells remained (Fig. 1).

To assess the degree of antigen selection and cell purity, we sorted 500 to 1000 cells from selected categories into reaction tubes and synthesized complementary DNA (cDNA) from $V_\beta 3$ mRNA, amplified them by the polymerase chain reaction (PCR), and then subcloned and sequenced them (Fig. 2). In the primary response, the junctional diversity in the TCRβ chain of activated T cells was highly restricted and exhibited many of the molecular hallmarks associated with PCC specificity in T cell lines and hybridomas (5, 8). In particular, 70% (21 out of 30) of the sequences from the primary activated population expressed the highly conserved asparagine at β100 together with $J_\beta 1.2$, versus 3 out of 53 clones from naïve animals and 3 out of 44 clones from

Table 1. Expansion of $V_\alpha 11^+V_\beta 3^+$ helper T cells expressing an N(N/S)A$^+$ TCR junctional sequence after primary and secondary injection with PCC (*29, 32*). Cell populations were sorted according to the phenotype of activation markers described and amplified $V_\beta 3$ DNA screened specifically for the N(N/S)A motif either by sequence analysis or by blots of $V_\beta 3^+$ DNA or $V_\beta 3^+$ colonies. The total number of N(N/S)A$^+$ cells in the original populations was calculated by use of the frequency obtained by the colony screen.

Sorted population ($V_\alpha 11^+V_\beta 3^+$)	Cells in lymph node (10^4)	Proportion of the N(N/S)A CDR3 loop motif			
		Total $V_\beta 3$ (%)			Total cells (*n*)
		Sequence	Dot blot	Colonies	
Naïve	2.7	<2.0	<1.0	0.05	14
Day 6 primary-unactivated	7.5	5.0	<1.0	0.2	150
Day 6 primary-activated	4.9	63.0	44.0	34.0	17,000
8 weeks post-primary	2.0	8.0	2.5	2.6	520
Day 6 memory-unactivated	4.6	<4.0	6.3	9.5	4,400
Day 6 memory-activated	4.8	80.0	75.0	69.0	33,000

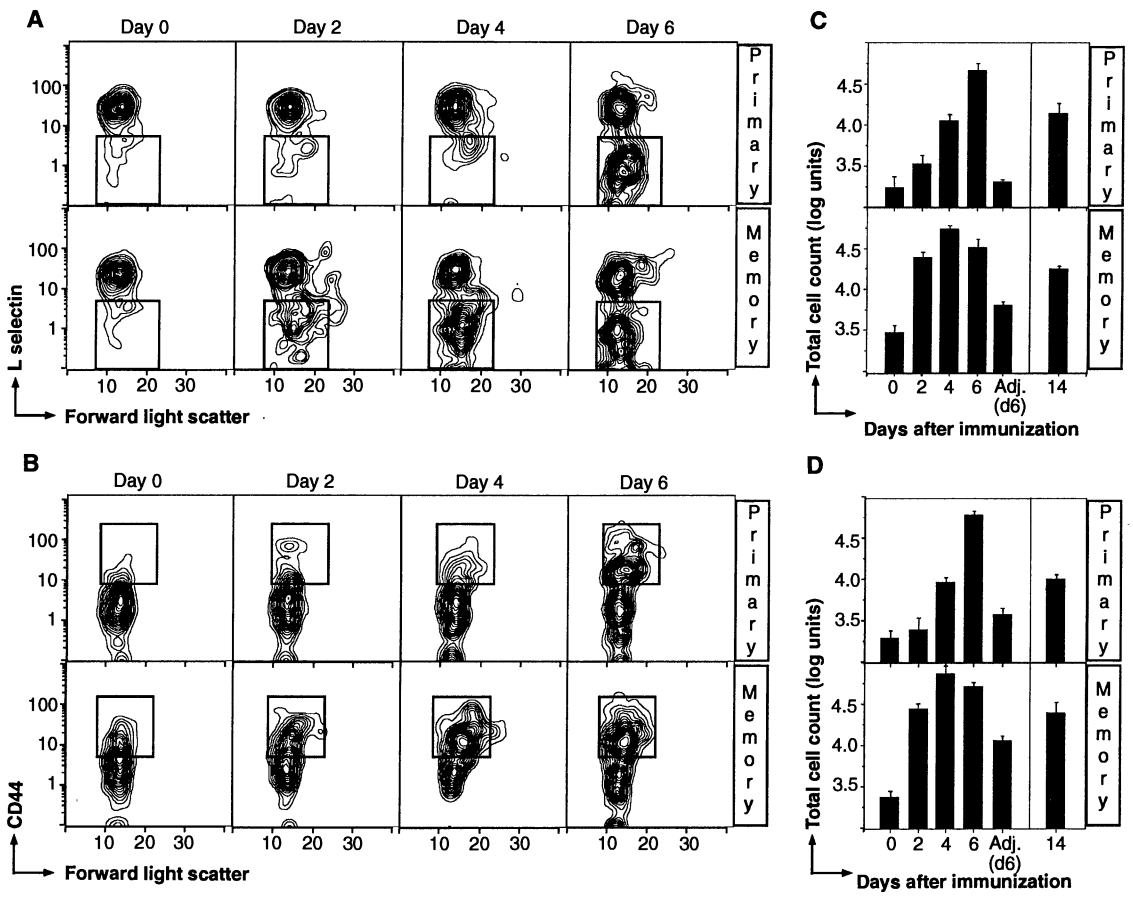

Fig. 1. Flow cytometric analysis of primary and memory helper T cells that react with PCC (*28*). All profiles show data on cells expressing $V_\alpha 11^+V_\beta 3^+$ that are negative for B220, CD11b, CD8, and propidium iodide staining (to exclude dead cells). More than 95 to 98% of these cells expressed CD4 at all stages of the response. Shown are changes in either L selectin (**A**) or CD44 (**B**) expression versus forward light scatter after PCC immunization. The total number of $V_\alpha 11^+V_\beta 3^+$ B220$^-$, CD11b$^-$, and CD8$^-$ cells in the draining lymph nodes are shown that expressed either low levels of L selectin (**C**) or high levels of CD44 (**D**); geometric means ± SD are presented for each time point [*n* = 5 for days 0 and 6 and *n* = 3 for days 2, 4, and 14, and day 6 adjuvant (Adj.) only for both primary and memory cells]. Units shown in (C) and (D) are logarithms of the actual values measured.

the nonactivated fraction. Another 20% of the clones expressed a threonine or serine residue at this position, indicating an alternative motif that has not been described previously. There was also a strong selection for alanine or glycine, two amino acids COOH-terminal to the asparagine (Fig. 2). We also observed a selection for a complementarity-determining region 3 (CDR3) loop of nine amino acids in length (100% of the sequences) (Fig. 2), confirming and extending the work of researchers who found a preponderance of $V_\beta 3$ transcripts of this size in unfractionated T cells after repeated immunization (9).

In the memory response, all but 2 of 41 sequences had asparagine at β100. All clones expressed an alanine or glycine at β102 and almost all had a CDR3 loop of nine amino acids and used $J_\beta 1.2$ (Fig. 2). The sequences in the primary response having a threonine or serine at position β100 were completely absent from this population. A series of 15 sequences from individual memory-activated cells displayed the same degree of restriction and a similar pattern of junctional sequence as found in the population analysis (Fig. 2). Control sequences from helper T cells that expressed $V_\alpha 11V_\beta 3$, isolated before either the first or second injection of PCC or from cells lacking the activated phenotype after injection, showed no evidence of selection and had a relatively random J_β usage and distribution of CDR3 lengths.

As population studies may have biases in terms of sequence representation, it would be useful to characterize α and β chains from single T cells. This would extend the analysis discussed above to give information on the complete heterodimer being selected. We therefore sorted individual T cells into tubes and amplified them by a "nested" PCR strategy (Fig. 3). We were able to sequence both TCR chains from 85% of single cells. Amplification of cDNA from single cells also avoids possible artifacts that are a result of PCR recombination (*10*). Our results (Fig. 3) show that the junctional diversity of TCRα chains from activated $V_\alpha 11V_\beta 3$ helper T cells are also highly restricted and have residues associated with PCC specificity in T cell lines and hybridomas (5). In particular, the glutamate residue at position α93 at the beginning of the CDR3 loop is thought to contact an exposed lysine of the cytochrome peptide (8). In the primary response, 70% of the T cells retain this residue, whereas in the memory response all responder cells with an eight–

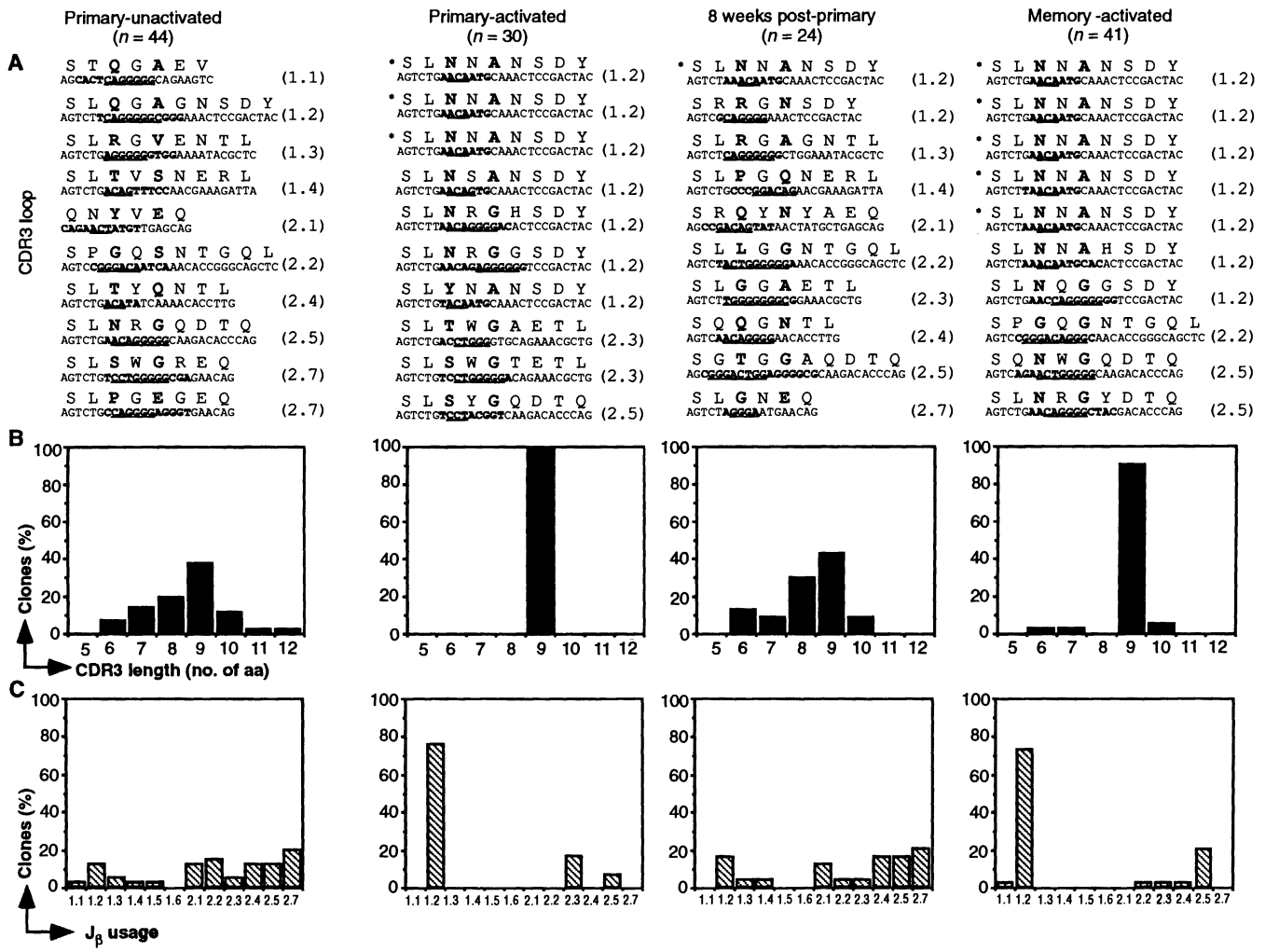

Fig. 2. $V_\beta 3$ junctional diversity profile of helper T cells indicates antigen-driven selection (*29, 30*). (**A**) A representative set of nucleotide and predicted amino acid sequences for the CDR3 loop of the $V_\beta 3$ gene from each sorted cell population. In each nucleotide sequence the most 5′ base pairs in plain text belong to the germline V region; then the next bold text represents N sequence additions flanking the germline D_β segments that are also bold but underlined; finally, the plain text that follows indicates base pairs from the germline J_β segment (in parentheses at the end of each sequence). The amino acid residues in bold indicate β chain position 100 and 102. The asterisk indicates an amino acid sequence identical to that of the PCC-specific clone 5C.C7. $V_\alpha 11V_\beta 3$ cells selected before injection with a resting phenotype (n = 53) expressed the same junctional profiles as the unactivated population. (**B**) Distribution of sequences from each population that express different lengths of the CDR3 loop as defined above; aa, amino acids. (**C**) Distribution of sequences from each population that express different J_β gene segments in association with $V_\beta 3$.

amino acid junction (12 out of 13) retain it. There is also a strong selection for serine (or the similar alanine, glycine, or threonine residue) at position α95. Furthermore, CDR3 length homogeneity is also evident, with a length of eight amino acids predominating in both the primary and memory responses (21 out of 24 clones) (Fig. 3). Both primary and memory responders use four of the same J_α segments (*TCRAJ 12, 21, 22,* and *34*), a significant degree of restriction because 50 J_α gene segments exist (*11*). Almost half of the cells in the memory response favored *TCRAJ 17* segments (6 out of 13 clones), whereas this J_α segment was not seen in any of the primary sequences.

In the β chains, we again saw the prevalence of asparagine at β100, the alanine or glycine at β102, the nine–amino acid length CDR3, and restricted J_β usage in both responses. $J_\beta 1.2$ usage was not as dominant as in the primary response, and $J_\beta 1.4$ usage appeared in conjunction with the β100 asparagine. This latter motif was not seen in the memory response. Overall, this single cell analysis corresponds well with the population analysis and further indicates the narrowing of TCR junctional diversity over the course of the response.

The predominant usage of a particular junctional amino acid sequence, N(N/S)A (where N is Asn, S is Ser, and A is Ala) (Fig. 2) (*9, 12*), allows us to quantitate the expansion and contraction of this PCC-responsive compartment of cells in a unique way. Using an oligonucleotide probe for the N(N/S)A junctional motif, we estimated the abundance of this sequence as a percentage of total $V_\beta 3$ DNA (dot blot) and as a frequency of total $V_\beta 3^+$ molecules (with the use of colony screens) (Table 1). Although TCR mRNA levels may change upon activation, the resting and activated cells are isolated independently and thus the ratios obtained by colony hybridization can be used as an indicator of the mRNA distribution in the original populations. Where comparable, there is a good correlation between the "dot blot" and colony screen analyses, and both of these correspond to the $N(N/S)A^+$ frequencies obtained by sequencing (Table 1). Our estimate for PCC-specific T cell precursors in naïve and "8 weeks post-primary" animals (Table 1) assumes the presence of an appropriate $V_\alpha 11$ chain and thus may be an overestimate. In any case, these data indicate that the total number of $V_\alpha 11V_\beta 3$ helper T cells expressing an N(N/S)A junctional motif increases by a factor of at least 1200 over the first 6 days of the primary response (Table 1). The frequency of this clonotype rose from 4.0×10^{-5} to 1.5×10^{-3} of total helper T cells in the draining lymph nodes (the total number of helper T cells increased by a factor of 2.4 over the same period). Eight weeks later, only 3% of these cells remained, representing a 40-fold expansion compared to that seen in the naïve cells. With the second injection of PCC, there was another 60-fold increase and 70% of the memory response clones expressed this motif compared to 35% of the primary clones (Table 1).

Thus, antibodies to the cell surface markers of activation together with those specific for the dominant TCR V_α and V_β gene segments allow the direct quantification of very rare populations of antigen-activated cells. The subsequent molecular analysis indicates that virtually all of these T cells have been selected for antigen

A

Clone		V	CDR3 loop	J	CDR3 (aa)	J
5C.C7	α	CAA TGTGCTGCT	EASNTNKV GAGGCTTCCAATACCAACAAAGTC	VFG GTCTTTGGA	8	34
	β	CAS TGTGCCAGC	SLNNANSDY AGTCTGAACAATGCAAACTCCGACTAC	TFG ACCTTCGGC	9	1.2
P.1	β	CAS TGTGCCAGC	SLNSANSDY AGTCTGAACAGTGCAAACTCCGACTAC	TFG ACCTTCGGC	9	1.2
P.2	α	CAA TGTGCTGCT	EAANTNKV GAGGCCGCCAATACCAACAAAGTC	VFG GTCTTTGGA	8	34
	β*	CAS TGTGCCAGC	SLNNANSDY AGTCTAAACAATGCAAACTCCGACTAC	TFG TTTTCGGT	9	1.2
P.3	α	CAA TGTGCTGCT	EALSNYNVL GAGGCTTTGTCTAATTACAACGTGCTT	YFG TACTTCGGA	9	21
	β	CAS TGTGCCAGC	SLSRANERL AGTCTCTCCAGAGCGAACGAAAGATTA	FFG TTTTCGGT	9	1.4
P.4	α	CAA TGTGCTGCT	GSSGSWQL GGGTCTTCTGGCAGCTGGCAACTC	IFG ATCTTTGGA	8	22
P.5	β	CAS TGTGCCAGC	SLNFSNERL AGTCTGAACTTTTCCAACGAAAGATTA	FFG TTTTCGGT	9	1.4
P.6	α	CAA TGTGCTGCT	AGGYNQGKL GCCGGGGGGTTATAACCAGGGGAAGCTT	IFG ATCTTTGGA	9	23
	β	CAS TGTGCCAGC	SGGRGTETL AGTGGGGGGCGCGGGACAGAAACGCTG	YFG TATTTTGGC	9	2.3
P.7	α	CAA TGTGCTGCT	EAAGGYKV GAGGCGGCTGGAGGCTATAAAGTG	VFG GTCTTTGGA	8	12
	β	CAS TGTGCCAGC	SLNRGQDTQ AGTCTGAACAGGGGCCAAGACACCCAG	YFG TACTTTGGG	9	2.5
P.8	α	CAA TGTGCTGCT	EPSSGQKL GAGCCTTCAAGTGGCCAGAAGCTG	VFG GTTTTTGGC	8	16
	β	CAS TGTGCCAGC	SLNRGKDTQ AGTCTGAACAGGGGGAAAGACACCCAG	YFG TACTTTGGG	9	2.5
P.9	α	CAA TGTGCTGCT	ETSSGQKL GAGACTTCAAGTGGCCAGAAGCTG	VFG GTTTTTGGC	8	16
	β	CAS TGTGCCAGC	SLNRGQDTQ AGTCTCAACAGGGGCCAAGACACCCAG	YFG TACTTTGGG	9	2.5
P.10	α	CAA TGTGCTGCT	EMSNYNVL GAGATGTCTAATTACAACGTGCTT	YFG TACTTCGGA	8	21
P.11	β	CAS TGTGCCAGC	SLNWGQDTQ AGTCTGAACTGGGGCCAAGACACCCAG	YFG TACTTTGGG	9	2.5
P.12	α	CAA TGTGCTGCT	EPSGSWQL GAGCCTTCTGGCAGCTGGCAACTC	IFG ATCTTTGGA	8	22
	β	CAS TGTGCCAGC	SLNRGQDTQ AGTCTCAACAGGGGCCAAGACACCCAG	YFG TACTTTGGG	9	2.5

B

Clone		V	CDR3 loop	J	CDR3 (aa)	J
M.1	α	CAA TGTGCTGCT	EASAGNKL GAGGCAAGTGCAGGGAACAAGCTA	TFG ACTTTTGGA	8	17
	β*	CAS TGTGCCAGC	SLNNANSDY AGTCTGAACAATGCAAACTCCGACTAC	TFG ACCTTCGGC	9	1.2
M.2	α	CAA TGTGCTGCT	EHSAGNKL GAGCACAGTGCAGGGAACAAGCTA	TFG ACTTTTGGA	8	17
M.3	β*	CAS TGTGCCAGC	SLNNANSDY AGTCTGAACAATGCAAACTCCGACTAC	TFG ACCTTCGGC	9	1.2
M.4	α	CAA TGTGCTGCT	ENSAGNKL GAGCACAGTGCAGGGAACAAGCTA	TFG ACTTTTGGA	8	17
M.5 M.6	β*	CAS TGTGCCAGC	SLNNANSDY AGTCTCAACAATGCAAACTCCGACTAC	TFG ACCTTCGGC	9	1.2
M.7	α	CAA TGTGCTGCT	EPSNYNVL GAGCCGTCTAATTACAACGTGCTT	YFG TACTTCGGA	8	21
	β	CAS TGTGCCAGC	SLNSANSDY AGTCTGAACAGTGCAAACTCCGACTAC	TFG ACCTTCGGC	9	1.2
M.8	α	CAA TGTGCTGCT	ESSGSWQL GAGTCTTCTGGCAGCTGGCAACTC	IFG ATCTTTGGA	8	22
	β	CAS TGTGCCAGC	SLNSANSDY AGTCTGAACAGTGCAAACTCCGACTAC	TFG ACCTTCGGC	9	1.2
M.9	α	CAA TGTGCTGCT	EVSGYNKL GAGGTCTCGGGATACAACAAACTC	TFG ATCTTTGGA	8	11
	β	CAS TGTGCCAGC	SLNWGQDTQ AGTCTGAACTGGGGGCAAGACACCCAG	YFG TACTTTGGG	9	2.5
M.10	α	CAA TGTGCTGCT	EAAGGYKV GAGGCGGCTGGAGGCTATAAAGTG	VFG GTCTTTGGA	8	12
	β	CAS TGTGCCAGC	SQNRGQDTQ AGCCAAAACAGGGGGCAAGACACCCAG	YFG TACTTTGGG	9	2.5
M.11	α	CAA TGTGCTGCT	EATSNNRI GAGGCGACTAGCAATAACAGAATC	FFG TTCTTTGGT	8	31
	β	CAS TGTGCCAGC	SPNRGQDTQ AGTCCAAACAGGGGGCAAGACACCCAG	YFG TACTTTGGG	9	2.5
M.12	α	CAA TGTGCTGCT	SNTNKV TCCAATACCAACAAAGTC	VFG GTCTTTGGA	6	34

Fig. 3. Single-cell PCR analysis of primary and memory T cells (*30, 31*). $V_\alpha 11$ and $V_\beta 3$ junctional diversity profiles of individually sorted $V_\alpha 11^+V_\beta 3^+$ L selectin^{hi} and CD44^{lo} cells from day 6 of the primary (**A**) or day 6 of the memory response (**B**). J_α gene segment assignment follows the nomenclature of Koop *et al.* (*11*). N sequence additions at the $V_\alpha J_\alpha$, $V_\beta D_\beta$, and $D_\beta J_\beta$ borders are in bold. All sequences are $V_\beta 3$ (the asterisk indicates a $V_\beta 3$ sequence with the 5C.C7 amino acid sequence) and $V_\alpha 11.1$ (except cell M.11, which is $V_\alpha 11.2$). Some α sequences contain no N sequence and imprecise $V_\alpha J_\alpha$ joints (the germline 3′ V_α sequence is TGTGCTGCTGAG). CDR3 length in amino acids and J_β and J_α assignment are also listed.

specificity. This degree of purity has not been achieved with any previously used immunohistochemical (*13*) or flow cytometric approaches (*14*). The extent of clonal expansion seen in this primary response is far greater than suggested by either bulk culture or limiting dilution analyses of other helper T cell responses to protein (*15*). It also exceeds that seen in the adoptive transfer model of Jenkins and colleagues (*16*), where the initial frequency of TCR transgenic T cells is at least 100 times greater than our estimate for PCC-specific T cell precursors in the normal animal. The expansion and contraction in activated cells is consistent with the rapid increase and decline of an effector T cell population seen in in vitro assays (*15*) and in the adoptive transfer model (*16*) and reiterates the kinetics of many $CD8^+$ T cell responses (*17*). The rapid decline in responsive cells is probably a result of both programmed cell death and outward migration (*18*). Furthermore, the retention of an increased number of antigen-specific T cells is compatible with the establishment of a long-lived memory compartment (*19*) that responds more quickly to a secondary challenge with antigen (*20*).

The fact that homogeneity in CDR3 length precedes sequence homogeneity in both TCR chains may relate to the strong influence that loop length has on the overall shape and packing of these structures on the basis of analyses of antibodies (*21*). Restriction of CDR3 length has also been noted in the selection of antigen-specific B cell memory (*10*). This CDR3 length homogeneity preceded diversification by somatic hypermutation (*10*). This CDR3 length homogeneity in TCRs may also provide a useful clue to the identification of specific responder cells to other antigens. Similarly, others (*22*) have recently identified CDR3 length and sequence restrictions in TCRβ chains from CD8 T cells responsive to human immunodeficiency virus.

We also see evidence for progressive clonal selection (*23*) during the evolution of antigen-specific T cell help in vivo. In particular, many T cells in the primary response have a small side-chain amino acid (glycine or alanine) at α93 (Fig. 3). A T cell hybridoma having a glycine at α93 was found to be broadly cross-reactive to most substitutions at position 99 of cytochrome c (*8*, *24*). This suggests that the change in the repertoire seen here may represent a selection for T cells expressing a receptor with greater specificity for the antigen–major histocompatibility complex (*25*). In contrast to Zheng *et al.* (*26*), we see no evidence for somatic hypermutation in the TCRα chain. Our data on $V_\alpha 11$ sequences derive from single activated T cells, all with productively rearranged and expressed TCRα chains paired with a TCRβ chain and expressing motifs associated with antigen specificity. Therefore, if somatic hypermutation occurs, it does not seem to affect either the cells studied here or the many hybridoma and cell lines reported previously (*12*, *27*).

REFERENCES AND NOTES

1. F. Celada, *Prog. Allergy* **15**, 223 (1971); P. C. Beverley, *Curr. Top. Microbiol. Immunol.* **159**, 111 (1990); S. L. Swain *et al.*, *Immunol. Rev.* **123**, 115 (1991); C. R. Mackay, *Adv. Immunol.* **53**, 217 (1993); J. Sprent, *Cell* **76**, 315 (1994).
2. I. C. MacLennan and D. Gray, *Immunol. Rev.* **91**, 61 (1986); K. Hayakawa, R. Ishii, K. Yamasaki, T. Kishimoto, R. R. Hardy, *Proc. Natl. Acad. Sci. U.S.A.* **84**, 1379 (1987); J. Jacob, R. Kassir, G. Kelsoe, *J. Exp. Med.* **173**, 1165 (1991); M. G. McHeyzer-Williams, G. J. V. Nossal, P. A. Lalor, *Nature* **350**, 502 (1991).
3. K. Matsui *et al.*, *Science* **254**, 1788 (1991); S. Weber, A. Traunecker, F. Oliveri, W. Gerhard, K. Karjalainen, *Nature* **356**, 793 (1992); Y. Sykulev *et al.*, *Immunity* **1**, 15 (1994).
4. G. Corradin and J. M. Chiller, *J. Exp. Med.* **149**, 436 (1979); S. M. Hedrick *et al.*, *Cell* **30**, 141 (1982); R. H. Schwartz, *Annu. Rev. Immunol.* **3**, 237 (1985).
5. S. M. Hedrick *et al.*, *Science* **239**, 1541 (1988).
6. A. M. Pullen, P. Marrack, J. W. Kappler, *Nature* **335**, 796 (1988); S. C. Jameson *et al.*, *J. Immunol.* **147**, 3185 (1991).
7. W. M. Gallatin, I. L. Weissman, E. C. Butcher, *Nature* **304**, 30 (1983); R. C. Budd *et al.*, *J. Immunol.* **138**, 3120 (1987).
8. J. L. Jorgensen *et al.*, *Nature* **355**, 224 (1992); J. L. Jorgensen, P. A. Reay, E. W. Ehrich, M. M. Davis, *Annu. Rev. Immunol.* **10**, 835 (1992).
9. M. Cochet *et al.*, *Eur. J. Immunol.* **22**, 2639 (1992).
10. M. G. McHeyzer-Williams, M. J. McLean, P. A. Lalor, G. J. V. Nossal, *J. Exp. Med.* **178**, 295 (1993); J. E. Ford, M. G. McHeyzer-Williams, M. R. Lieber, *Gene* **142**, 279 (1994); J. E. Ford, M. G. McHeyzer-Williams, M. R. Lieber, *Eur. J. Immunol.* **24**, 1816 (1994).
11. B. F. Koop *et al.*, *Genomics* **19**, 478 (1994).
12. P. J. Fink, L. A. Matis, D. L. McElligott, M. Bookman, S. M. Hedrick, *Nature* **321**, 219 (1986).
13. K. A. Fuller, O. Kanagawa, M. H. Nahm, *J. Immunol.* **151**, 4505 (1993).
14. H. R. MacDonald, J. L. Casanova, J. L. Maryanski, J. C. Cerottini, *J. Exp. Med.* **177**, 1487 (1993); S. L. Reiner, Z.-E. Wang, F. Hatam, P. Scott, R. M. Locksley, *Science* **259**, 1457 (1993).
15. A. Kelso *et al.*, *Immunol. Rev.* **123**, 85 (1991); L. M. Bradley, D. D. Duncan, S. Tonkonogy, S. L. Swain, *J. Exp. Med.* **174**, 547 (1991); S. L. Swain and L. M. Bradley, *Semin. Immunol.* **4**, 59 (1992).
16. K. R. Kearney, K. A. Pape, D. Y. Loh, M. K. Jenkins, *Immunity* **1**, 327 (1994).
17. J. C. Cerottini and H. R. MacDonald, *Annu. Rev. Immunol.* **7**, 77 (1989); R. Ahmed, *Semin. Immunol.* **4**, 105 (1992); S. Oehen, H. Waldner, T. M. Kundig, H. Hengartner, R. M. Zinkernagel, *J. Exp. Med.* **176**, 1273 (1992); R. M. Zinkernagel *et al.*, *Immunol. Rev.* **133**, 199 (1993); S. Hou and P. C. Doherty, *J. Immunol.* **150**, 5494 (1993); S. Hou, L. Hyland, K. W. Ryan, A. Portner, P. C. Doherty, *Nature* **369**, 652 (1994); L. L. Lau, B. D. Jamieson, T. Somasundaram, R. Ahmed, *ibid.*, p. 648.
18. J. Sprent, *Cell. Immunol.* **21**, 278 (1976); S. Webb, C. Morris, J. Sprent, *Cell* **63**, 1249 (1990); Y. Kawabe and A. Ochi, *Nature* **349**, 245 (1991); D. Moskophidis, F. Lechner, H. Pircher, R. M. Zinkernagel, *ibid.* **362**, 758 (1993).
19. D. F. Tough and J. Sprent, *J. Exp. Med.* **179**, 1127 (1994); J. Sprent and D. F. Tough, *Science* **265**, 1395 (1994).
20. L. M. Bradley, D. D. Duncan, K. Yoshimoto, S. L. Swain, *J. Immunol.* **150**, 3119 (1993).
21. E. A. Padlan, *Q. Rev. Biophys.* **10**, 1 (1977); C. Chothia *et al.*, *Nature* **342**, 877 (1989).
22. G. Pantaleo *et al.*, *Nature* **370**, 463 (1994).
23. F. M. Burnet, *The Clonal Selection Theory of Acquired Immunity* (Cambridge Univ. Press, Cambridge, MA, 1959).
24. P. A. Reay, J. L. Jorgensen, M. M. Davis, in preparation.
25. Such an increase in specificity would also imply an increase in affinity, although not necessarily on the same scale as that seen with antibodies.
26. B. Zheng, W. Xue, G. Kelsoe, *Nature* **372**, 556 (1994).
27. Y. Chien *et al.*, *ibid.* **309**, 322 (1984); U. Wurzburg, H. Schutt-Gerowitt, K. Rajewsky, *Eur. J. Immunol.* **3**, 762 (1973); R. K. Barth *et al.*, *Nature* **316**, 517 (1985); M. Kronenberg, G. Siu, L. Hood, N. Shastri, *Annu. Rev. Immunol.* **4**, 529 (1986); E. S. Vitetta *et al.*, *ibid.* **9**, 193 (1991).
28. B10.BR mice (6 to 10 weeks old) were immunized subcutaneously with 200 μg of PCC (Sigma) in 100 μg of RIBI adjuvant (ImmunoChem Research, Hamilton, MT) or adjuvant alone, 100 μl on each side of the base of the tail; secondary injections were given after 8 weeks. T cells isolated from inguinal and periaortic lymph nodes were stained with the biotinylated antibody, then stained with Texas Red–avidin together with fluoresceinated, phycoerythrin- and allophycocyanin-labeled antibodies and then placed in 1 μg/ml propidium iodide. This was done with the appropriate combinations of biotinylated Pgp-1 [antibody to CD44 (anti-CD44); Pharmingen, San Diego] and MEL-14 (anti–L selectin; Pharmingen); fluorescein-labeled R.R 8-1 (anti-$V_\alpha 11$; Pharmingen); phycoerythrin-labeled 6B2 (anti-B220; Pharmingen), 53-6.7 (anti-CD8), and MAC-1 (anti-CD11b); and allophycocyanin-labeled KJ25 (anti-$V_\beta 3$). Cells were analyzed with a FACS 440 (Becton Dickinson, San Jose, CA) with dual laser capability; 300,000 events were collected in list mode with each file gated on propidium iodide (excluded in the phycoerythrin channel), forward scatter, and obtuse light scatter to exclude erythrocytes and most dead cells. All profiles are represented as 5% probability contour plots (distribution profiles of 300 to 900 cells in total).
29. Cells were selected from two animals in each group as described (*28*). The 8 weeks post-primary $V_\alpha 11V_\beta 3$ population (and the resting cell population) was selected as $CD4^+$ and $B220^-$, $CD11b^-$, and $CD8^-$. The cells from animals 6 days after injection were costained for L selectin (biotin-conjugated and stained with avidin–Texas Red; Pharmingen) and CD44 (phycoerythrin conjugate; Pharmingen) together with antibodies to $V_\alpha 11$ and $V_\beta 3$ and selected as activated if they expressed both low levels of L selectin and high levels of CD44; unactivated populations expressed high levels of L selectin and low levels of CD44; CDR3 loop length was counted two amino acids downstream from the conserved cysteine in the V region to two amino acids upstream from the conserved GXG motif (where G is Gly and X is any amino acid) in the J region as described [E. P. Rock, P. R. Sibbald, M. M. Davis, Y.-H. Chien, *J. Exp. Med.* **179**, 323 (1994)]. Gated cells (500 to 1000) (in one experiment four memory-activated cells per tube; $n = 15$) were sorted directly into tubes containing 25 μl of cDNA synthesis reaction mixture as described [H. Chang *et al.*, *J. Immunol.* **143**, 315 (1989)], using oligonucleotide primers specific for C_β (TTACCGTTCCTCCAGGTGTC) (C_β.1) and C_α (GTTTTGTCAGTGATGAACGT) (C_α.1). Five microliters of the cDNA reaction was used for 35 cycles of a 20-μl PCR reaction with standard buffer conditions and 2 mM final Mg^{2+} concentration, with 30 s of melting at 92°C, 45 s of annealing at 55°C, and 90 s of extension at 70°C; for this, we used primers specific for the $V_\beta 3$ leader.1 sequence (CTGGGTGCAAGAATTTTG) ($V_\beta 3$.L1) and the same C_β.1 primer as above. Two microliters of the first-round PCR reaction was re-amplified for 35 more cycles under the same conditions with the use of a "nested" pair of primers for the C_β (AAGAAGGGACTGGTGCAC) (C_β.2) and $V_\beta 3$ leader (ATGGCTACAAGGCTCTGGTA) ($V_\beta 3$.L2). One microliter of second-round PCR product was ligated into pGEM-T as recommended (Promega, Madison, WI). Two microliters of the liga-

tion reaction was used to transform *Escherichia coli* [C. L. Hseih *et al.*, *Mol. Cell. Biol.* **11**, 3972 (1991)] by electroporation; the bacteria were grown overnight on agar plates containing ampicillin (100 μg/ml; Sigma). Colonies were expanded for plasmid DNA isolation and double-stranded DNA sequencing with the use of PRISM Ready Reaction Dyedeoxy Terminator Cycle sequencing reactions as recommended by the supplier (Applied Biosystems, Foster City, CA) with a $V_\beta3$ primer (CTCTGCTGAGTGTCCTTCAA) ($V_\beta3.2$); we then performed gel electrophoresis with detection and analysis of the fluorescent product using the Applied Biosystems model 373A DNA sequencing system. No repeat sequences were found in either the naive resting group or the unactivated populations; one of 24 sequences was repeated in the 8 weeks post-primary group [and this bore the typical NNA motif (where N is Asn and A is Ala) of PCC reactivity]. Many repeats were found in both activated groups. In the primary-activated group, 11 unique sequences were found among the 30 clones; of these sequences, four were repeated 12, 6, 3, and 2 times. In the memory-activated group, there were eight unique sequences of the 26 clones from the population analysis; of these, four were repeated 12, 5, 3, and 2 times. Of the 15 single cells, there were 10 unique sequences, two of which were repeated 5 and 2 times.

30. Abbreviations for the amino acid residues are A, Ala; C, Cys; D, Asp; E, Glu; F, Phe; G, Gly; H, His; I, Ile; K, Lys; L, Leu; M, Met; N, Asn; P, Pro; Q, Gln; R, Arg; S, Ser; T, Thr; V, Val; W, Trp; and Y, Tyr.
31. Immunization, staining for flow cytometry, cell sorting, cDNA synthesis, PCR, "nested" PCR, and DNA sequencing were undertaken as described (*29*) with variations as follows. Individual cells were sorted into tubes containing 5 μl of cDNA reaction mix with the use of oligo(dT) for priming (Becton Dickinson Labware, Bedford, MA). All 5 μl of the cDNA reaction was used for the first 35 cycles of PCR with β chain–specific primers $C_\beta.2$ and $V_\beta3.L.2$ (*29*) together with a C_α-specific primer (GTTTTGTCAGTGATGAACGT) ($C_\alpha.1$) and $V_\alpha11$ leader–specific primer (ATGCAGAGGAACCTGGGAGC) ($V_\alpha11.L1$). For the second 35 cycles of PCR, "nested" primers for each chain were used in separate reactions: C_β-specific (AATCTGCAGCACGAGGGTAGCCTTTTG) ($C_\beta.3$) and $V_\beta3$-specific (AATCTGCAGAATTCAAAAGTCATTCAG) ($V_\beta3.1$) for the TCRβ chain and C_α-specific (AATCTGCAGCGGCACATTGATTTGGGA)($C_\alpha.2$) and $V_\alpha11$ leader–specific (AATCTGCAGTGGGTGCAGATTTGCTGG) ($V_\alpha1.12$) for the TCRα chain. The primer $V_\beta3.2$ (*29*) and one specific for C_α (GGCGTCGTCGACGAACAGGCAGAGGGTGCTGTCCTGAG) ($C_\alpha.3$) were used for direct sequencing of the PCR product after column separation of PCR product from primers.
32. Animals were immunized and populations sorted by phenotype as described (*29*). "Sequence" in Table 1 shows a summary from data presented in Fig. 2. "Dot blot" shows the results from screening PCR products containing $V_\beta3$-amplified DNA from the sorted populations as described (*29*). These products were titrated onto Hybond N (Amersham, Arlington Heights, IL) nylon filters and probed with ^{32}P kinase-labeled oligonucleotide specific for the N(N/S)A sequence and three nucleotides in each of $V_\beta3$ and $J_\beta1.2$ (CTGAACAATGCAAAC) and subsequently with an oligonucleotide specific for all $V_\beta3$ sequences (primer: $V_\beta3.2$) (*29*) under conditions where only 2 base pairs of mismatch was tolerated, with hybridization at 54°C and washing at 58°C in 3 M tetramethylammonium chloride solution as described [R. P. Dong *et al.*, *Tissue Antigens* **39**, 106 (1992)]. Filters were exposed to a phosphor screen and quantified on a Molecular Dynamics PhosphoImager with ImageQuant software (Molecular Dynamics, Sunnyvale, CA). "Colonies" in Table 1 shows the results after subcloning PCR products from the sorted populations (*29*). The colonies were then transferred onto Hybond N and probed with the same labeled oligonucleotide in 30% formamide containing 3× SSPE hybridization solution at 42°C for 5 hours, and washed finally in 0.2% SSPE at 30°C. Overall, this mode of analysis greatly increased the size of sample screened from each population (500 to 4000 $V_\beta3^+$ colonies screened) and gave similar results from two independent screens of clones derived from separate ligation reactions. We estimated the total cell counts by extrapolating the frequency obtained by the colony lift assay to the total cell counts estimated by flow cytometric analysis (as described in Fig. 1) for cells with the appropriate phenotype.
33. We would like to thank J. Ford, Y.-h. Chien, A. Kantor, C. Goodnow, J. Cyster, and E. Rock for many constructive comments regarding this work. We also thank F. Baker, D. Mack, Y. Fukui, J. Altman, and P. Lu for expert technical advice and helpful discussions. Supported by funds from the Howard Hughes Medical Institute (M.M.D.), M.McH.-W. is a fellow of the Lucille P. Markey Charitable Trust.

13 October 1994; accepted 9 January 1995

Processing of Complex Sounds in the Macaque Nonprimary Auditory Cortex

Josef P. Rauschecker,*† Biao Tian,† Marc Hauser

Neurons in the superior temporal gyrus of anesthetized rhesus monkeys were exposed to complex acoustic stimuli. Bandpassed noise bursts with defined center frequencies evoked responses that were greatly enhanced over those evoked by pure tones. This finding led to the discovery of at least one new cochleotopic area in the lateral belt of the nonprimary auditory cortex. The best center frequencies of neurons varied along a rostrocaudal axis, and the best bandwidths of the noise bursts varied along a mediolateral axis. When digitized monkey calls were used as stimuli, many neurons showed a preference for some calls over others. Manipulation of the calls' frequency structure and playback of separate components revealed different types of spectral integration. The lateral areas of the monkey auditory cortex appear to be part of a hierarchical sequence in which neurons prefer increasingly complex stimuli and may form an important stage in the preprocessing of communication sounds.

In 1973, Merzenich and Brugge described several auditory areas on the supratemporal plane (STP) of the macaque brain, surrounding primary auditory cortex AI (*1*). One of these areas, which they termed L, extends laterally alongside AI and onto the exposed lateral surface of the superior temporal gyrus (STG). Anatomically, several areas have been identified in this region on the basis of cyto-, myelo-, and chemoarchitecture (*2–4*). In particular, the term "belt" has been introduced to characterize the cortical region that adjoins the koniocortical primary area laterally (*2*). Little is known about the functional properties of neurons in any nonprimary auditory cortical areas of the monkey, because these neurons tend to respond poorly and inconsistently to conventional pure-tone (PT) stimuli (*5*).

Neurons in the nonprimary visual cortex similarly do not respond well to small stationary spots of light. Extrastriate neurons have larger receptive fields and prefer more complex stimuli than do neurons in the striate cortex (*6*) because they integrate visual information spatially over a larger range. By the same token, auditory neurons that are higher up in the processing pathway might be expected to integrate information over a larger range of frequencies. We therefore used one set of auditory stimuli that consisted of bandpassed noise (BPN) bursts with variable bandwidth around a given center frequency. This type of stimulus is directly analogous to a bar or spot of light with variable size at a given receptive field position in the visual system. Thus, our experiments were designed to test for the existence of neurons that prefer a certain bandwidth of BPN bursts, just as neurons in the extrastriate cortex prefer a certain size of visual stimulus (*7*).

We selected a second type of auditory stimulus on the basis of the following considerations. In humans, the lateral surface of the STG includes areas 42 and 22 of Brodmann, which correspond to areas TB and TA, respectively, of von Economo (*8*). Lesions in these areas, especially in their posterior parts, cause deficits in speech perception but have relatively little effect on general auditory discrimination (*9*). Hence, from an evolutionary and comparative neuroanatomical perspective, it was of interest to include species-specific communication calls as another type of wide-band signal. Previous nonhuman primate studies of this type have been performed only with squirrel monkeys (*10*).

Electrode penetrations were made along both sides of the lateral fissure into the

J. P. Rauschecker and B. Tian, Laboratory of Neurophysiology, National Institute of Mental Health, Poolesville, MD 20837, USA.
M. Hauser, Departments of Anthropology and Psychology, Program in Neuroscience, Harvard University, Cambridge, MA 02138, USA.

*To whom correspondence should be addressed.
†Present address: Laboratory of Neuropsychology, National Institute of Mental Health, Building 49, Room 1B80, Bethesda, MD 20892–4415, USA.